Sum Rate optimization for RIS-Aided RSMA system with Movable Antenna

Mingyu Hu *, Nan Liu + and Wei Kang *
*School of Information Science and Engineering, Southeast University, Nanjing, China 210096
+National Mobile Communications Research Laboratory, Southeast University, Nanjing, China 210096
{myuhu, nanliu, wkang}@seu.edu.cn

arXiv:2512.23242v2 [cs.IT] 10 Mar 2026

***Abstract*—Rate-Splitting Multiple Access (RSMA) is a key enabling technique for sixth-generation (6G) wireless systems due to its powerful interference management, and Reconfigurable Intelligent Surface (RIS) improves communication performance by shaping wireless propagation. However, conventional RSMA–RIS architectures employ fixed antennas, limiting spatial degrees of freedom and system performance. To address this, we propose a movable-antenna (MA) assisted RSMA–RIS framework and formulate a sum-rate maximization problem that jointly optimizes the transmit beamforming matrix, RIS reflection matrix, common-rate partition, and MA positions. After yielding a closed-form solution for common rate splitting, the problem is transformed via fractional programming (FP). Using Karush–Kuhn–Tucker (KKT) conditions, we give iterative updates for Lagrange multipliers and beamforming matrix, obtain the RIS reflection matrix via the dual problem, and determine optimal antenna positions via gradient ascent. Numerical results show that with the existence of RIS, integrating MA yields additional gains of approximately 33.3% for SDMA and 35.6% for RSMA.**

***Index Terms*—Rate-splitting multiple access (RSMA), reconfigurable intelligent surface (RIS), movable antenna (MA), Karush–Kuhn–Tucker (KKT) conditions.**

I. Introduction

Movable antenna (MA) has recently emerged as a promising technique delivering substantial performance gains in wireless systems [1]. By connecting each radiating element to the RF chain via a flexible coaxial cable [2], MA enables adaptive repositioning within a multi-wavelength region, thereby expanding spatial degrees of freedom, supporting high-quality beamforming, and reducing hardware cost relative to antenna selection (AS) schemes. Unlike conventional fixed-position antennas (FPAs) restricted to 1D/2D layouts, MA exploits full 3D spatial flexibility. These advantages have been validated across diverse scenarios. Demonstrated in [3], the deployment of movable antenna (MA) yields significant capacity gains in multiple-input multiple-output (MIMO) systems. The authors of [4] extend the performance enhancement of MA for MIMO systems to the case of statistical channel conditions. Moreover, the performance enhancement of MAs in multiple access channels (MACs) was analyzed in [5]. Additionally, MAs have also been empirically verified to improve system performance in various other communication scenarios, such as enhancing the efficiency of mobile edge computing (MEC) systems [6] and enabling satisfactory secrecy performance in covert communication systems [7].

Rate-Splitting Multiple Access (RSMA) is a promising multiple-access scheme for next-generation wireless networks. It splits each user's message into a common part and a private part, encoded into one common stream and multiple private streams, respectively [8]. Each user first decodes the common stream by treating all private streams as noise, and then decodes its own private message after removing the common stream. Among various RSMA architectures, 1-layer RSMA is widely adopted due to its strong performance [9]. RSMA also enables robust interference management under diverse channel conditions. In particular, under weak or strong inter-user interference, it can adapt the common-private split and reduce to SDMA or NOMA, respectively [10]. Moreover, RSMA achieves higher degrees of freedom than SDMA and NOMA, yielding faster user-rate growth with the signal-to-noise ratio (SNR) [11], [12].

Reconfigurable intelligent surface (RIS) is a kind of metasurface technology consisting of a two-dimensional array of reflective elements, each of which can independently adjust the phase of the incident signal according to the instantaneous channel, thereby synthesizing highly directive reflected beams and enhancing system performance—especially when the line-of-sight (LoS) path between the base station (BS) and users is blocked or severely attenuated by obstacles. Extensive investigations on RIS have been performed across diverse deployment scenarios like in [13]–[15].

Typically, RSMA outperforms SDMA and NOMA when practical channels between the base station and users fall between the extremes of orthogonality and full alignment [8]. Since both MA and RIS can actively shape the effective channel, their benefits are expected to be more pronounced for RSMA. To the best of our knowledge, the performance gains of MAs for RSMA–RIS systems remain unexplored. Motivated by this gap, we propose a downlink multiuser MISO scheme with MA-assisted RSMA–RIS, wherein we maximize the sum rate by jointly optimizing the transmit beamforming matrix, the RIS reflection matrix, the common-rate partition, and the MA positions. The problem is recast via fractional programming (FP) into a more tractable form.

This work is partially supported by the National Natural Science Foundation of China under Grants 62361146853, and 62371129, and the Research Fund of the National Mobile Communications Research Laboratory, Southeast University, under Grant 2026A05.

Efficient updates are then derived using the Karush–Kuhn–Tucker (KKT) conditions and associated dual problem. Finally the antenna positions are obtained through a gradient-ascent procedure. Our main contributions are summarized as follows:

- To the best of our knowledge, this is the first work to investigate the performance gains of MA for RSMA–RIS system. We formulate a sum-rate maximization that jointly optimizes the transmit beamforming matrix, the RIS reflection matrix, the common-rate allocation, and the MA positions.
- We propose an effective alternating optimization (AO) iterative algorithm to solve the formulated optimization problem. Specifically, by decomposing the initial problem into several subproblems, each variables can be updated via corresponding approaches.
- Numerical results show that, MA can improve the performance of RSMA-RIS system compared with FPA. Also, the algorithm proposed in this work can effectively solve the initial problem and outperforms the benchmark algorithms.

II. System Model

In this paper, we consider the system shown in Fig. 1, where the BS is equipped with M movable antennas and adopts 1-layer RSMA to split user messages. The BS simultaneously serves K far-field single-antenna users in the presence of obstacles, which create non-line-of-sight (NLOS) paths. For simplicity, each antenna is allowed to move horizontally via flexible cables. In addition, a RIS with N reflecting elements is deployed to enhance communication performance.

A. Channel Model

In this work, the field response model in [3] is adopted for channel modeling. Let $\mathcal{M} = \{1, \cdots, M\}$ denote the set of MAs, with positions $\mathbf{x} = [x_1, x_2, \ldots, x_M]$, where x_m is the position of the m-th MA. The end-to-end channel consists of three components. First, we assume that the channel state information (CSI) of the RIS–user link, denoted by $\mathbf{h}_{r,k} \in \mathbb{C}^{N\times 1}$, is available at the BS. We consider a geometric channel model with L_t transmit paths from the BS and L_r receive paths at the RIS. The far-field response vector (FRV) from the BS to the RIS is defined as $\mathbf{a}(x_i) = [e^{j\frac{2\pi}{\lambda}x_i\cos\theta^t_1}, \cdots, e^{j\frac{2\pi}{\lambda}x_i\cos\theta^t_{L_t}}]^T \in \mathbb{C}^{L_t\times 1}$, where θ^t_i, $i \in \{1, 2, \ldots, L_t\}$, denotes the transmit angle of the i-th BS propagation path. Stacking all FRVs yields the field response matrix (FRM) $\mathbf{A}(\mathbf{x}) = [\mathbf{a}(x_1), \mathbf{a}(x_2), \cdots, \mathbf{a}(x_M)] \in \mathbb{C}^{L_t\times M}$. Similarly, the receive steering vector of the RIS is defined as $\mathbf{b}_i = [b_{i,1}, \cdots, b_{i,L_r}]^T$, where $b_{i,j} = e^{j\frac{2\pi}{\lambda}(x_{r,i}\sin\theta^r_j\cos\phi^r_j + y_{r,i}\cos\theta^r_j)}$, $(x_{r,i}, y_{r,i})$ is the coordinate of the i-th RIS element, and θ^r_i and ϕ^r_i are the corresponding elevation and azimuth angles at the RIS receive side. By stacking these vectors, we obtain $\mathbf{B} = [\mathbf{b}_1, \mathbf{b}_2, \cdots, \mathbf{b}_N] \in \mathbb{C}^{L_r\times N}$. The equivalent BS–RIS channel is $\mathbf{H}_{b,r}(\mathbf{x}) = \mathbf{B}^H\mathbf{\Sigma}\mathbf{A}(\mathbf{x})$, where $\mathbf{\Sigma} \in \mathbb{C}^{L_r\times L_t}$ is the BS–RIS fading matrix, and each entry $\mathbf{\Sigma}[i,j]$ denotes the fading coefficient between the i-th receive path and the j-th transmit path, following a complex Gaussian distribution. Similarly, the BS–user response matrix is $\mathbf{A}_k(\mathbf{x}) = [\mathbf{a}_k(x_1), \cdots, \mathbf{a}_k(x_M)]$, where $\mathbf{a}_k(x_i) = [e^{j\frac{2\pi}{\lambda}x_i\cos\theta^t_{k,1}}, \cdots, e^{j\frac{2\pi}{\lambda}x_i\cos\theta^t_{k,L_t}}]^T$ and $\theta^t_{k,i}$ denotes the transmit angle of the i-th BS–user k path. Accordingly, the BS–user channel is $\mathbf{h}^H_{b,k} = \mathbf{1}^H\mathbf{\Sigma}_k\mathbf{A}_k(\mathbf{x})$, where $\mathbf{1}$ is an all-one row vector and $\mathbf{\Sigma}_k \in \mathbb{C}^{L_r\times L_t}$ is the BS–user k fading matrix. Each entry $\mathbf{\Sigma}_k[i,j]$ denotes the fading coefficient between the i-th receive path and the j-th transmit path and also follows a complex Gaussian distribution. Therefore, the combined equivalent channel from the BS to user k is $\mathbf{h}^H_k(\mathbf{x}) = \mathbf{h}^H_{r,k}\mathbf{\Phi}\mathbf{H}_{b,r}(\mathbf{x}) + \mathbf{h}^H_{b,k}$, where $\mathbf{\Phi} = \mathrm{diag}([\phi_1, \cdots, \phi_N])$, and ϕ_i is the reflection coefficient of the i-th RIS element with $|\phi_i| = 1$ for all i, where $|\cdot|$ denotes the magnitude.

B. Signal Model

In a 1-layer RSMA, the message for user k which is denoted as W_k is divided into a common part $W_{c,k}$ and a private part $W_{p,k}$. The private part of each user is encoded into an independent private stream s_k for $k = 1, \cdots, K$. The common parts of each user are combined into one part and consequently encoded into s_c. It is assumed that each stream in $\mathbf{s} = \{s_1, s_2, ..., s_K, s_c\}$ satisfies $\mathbb{E}[s_i\bar{s}_i] = 1$ and $\mathbb{E}[s_i\bar{s}_j] = 0, \forall i \neq j$ [16]. $\bar{(\cdot)}$ denotes the conjugate. We denote the beamformer of the k-th private stream and the common stream as $\mathbf{w}_k$ and $\mathbf{w}_c$, respectively. Then we can define the beamforming matrix $\mathbf{W}$ as $\mathbf{W} = [\mathbf{w}_1, \cdots, \mathbf{w}_K, \mathbf{w}_c] \in \mathbb{C}^{M\times(K+1)}$. Therefore, the received signal at user k can be expressed as:

$$y_k = \mathbf{h}^H_k(\mathbf{x})\mathbf{W}\mathbf{s} + n_k, \tag{1}$$

where $n_k \sim \mathcal{CN}(0, \sigma^2_k)$ is the receiver noise of the user k. According to the 1-layer RSMA scheme, the user decodes the common stream while regarding other streams as interference. After canceling the common part from the stream, users proceed to decode their private parts. The signal-to-interference-plus-noise ratio (SINR) for decoding the common part at user k can be expressed as:

$$\mathrm{SINR}_{c,k} = \frac{|\mathbf{h}^H_k(\mathbf{x})\mathbf{w}_c|^2}{\sum_{i=1}^K |\mathbf{h}^H_k(\mathbf{x})\mathbf{w}_i|^2 + \sigma^2_k} \tag{2}$$

Consequently, we can get the maximum rate of user k for decoding common stream as:

$$R_{c,k} = \log_2(1 + \mathrm{SINR}_{c,k}) \tag{3}$$

To ensure that each user can correctly decode the common stream s_c, the sum of the allocated common rates, $\sum_k r_{c,k}$, should not exceed $\min_k\{R_{c,k}\}$, where $r_{c,k}$ is the common rate allocated to the user k. Then the SINR for decoding the private stream at the user k is given by:

$$\mathrm{SINR}_k = \frac{|\mathbf{h}^H_k(\mathbf{x})\mathbf{w}_k|^2}{\sum_{i=1, i\neq k}^K |\mathbf{h}^H_k(\mathbf{x})\mathbf{w}_i|^2 + \sigma^2_k} \tag{4}$$

Then, the maximum rate for decoding the private stream at user k is denoted as:

$$R_k = \log_2(1 + \mathrm{SINR}_k) \tag{5}$$

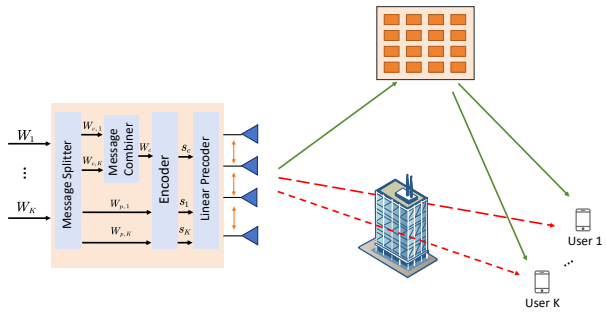

Fig. 1: System model of an MA-aided RSMA-RIS system.

C. Problem Formulation

To investigate whether MA can enhance system performance in the RSMA-RIS system, we formulate an optimization problem that aims to maximize the sum of both the private and common achievable rates of all users. The optimization problem is formulated as:

$$
\begin{aligned}
(\mathbf{P1}) \max_{\mathbf{x},\mathbf{W},\mathbf{\Phi},\{r_{c,k}\}} \quad & R = \sum_{k=1}^{K}(R_k + r_{c,k}) && \text{(6a)}\\
\text{s.t.} \quad & \text{tr}\left(\mathbf{W}^H\mathbf{W}\right) \le P_T, && \text{(6b)}\\
& R_k \ge \iota, \quad \forall k && \text{(6c)}\\
& \sum_{k=1}^{K} r_{c,k} \le R_{c,k}, \quad \forall k, && \text{(6d)}\\
& r_{c,k} \ge 0, \quad \forall k, && \text{(6e)}\\
& |\phi_i|^2 = 1, \quad \forall i, && \text{(6f)}\\
& X_{min} \le x_i \le X_{max}, && \text{(6g)}\\
& \|x_i - x_j\|_2 \ge D_0, \quad \forall i \ne j. && \text{(6h)}
\end{aligned}
$$

Constraint (6b) is the power constraint with P_T denoting the power budget of the BS, (6c) is the private rate constraint to ensure the fairness with ι the threshold for private rate, (6d) is the common rate constraint to make sure that every user can successfully encode the common stream, (6e) represents the non-negativity constraint of the common rate, (6f) represents the constant-modulus constraint imposed on each RIS element, (6g) represents the minimum inter-antenna spacing constraint with X_{min} and X_{max} the limits of region for MA, (6h) is the minimum distance between antennas with D_0 the minimum inter-antenna spacing between any two antennas.

Due to the non-convex nature of (6a), (6c), (6f) and (6h), as well as the strong coupling among the optimization variables, problem (**P1**) is a highly non-convex optimization problem. In the subsequent sections, we develop an efficient alternating optimization (AO) algorithm to solve this problem.

III. PROPOSED SOLUTION

In this section, we propose an efficient AO algorithm to solve problem (**P1**). Specifically, by fixing a subset of variables and optimizing the remaining ones, the original problem is decomposed into several tractable subproblems. Moreover, closed-form solutions are derived in some subproblems, which reduces the overall computational complexity.

A. Updating Allocated Common Rates

When all optimization variables except for the allocated common rate are fixed, the original problem can be transformed into:

$$
(\mathbf{P2}) \quad \max_{\{r_{c,k}\}} \sum_{k=1}^{K} r_{c,k} \quad \text{s.t. (6d), (6e)}
$$

where constraint (6d) can be equivalently rewritten as $\sum_{k=1}^{K} r_{c,k} \le \min_k\{R_{c,k}\}$. This reformulation indicates that the sum of the common-rate allocations assigned to all users cannot exceed the minimum achievable common rate among all users. Since the objective function is monotonically increasing with respect to $r_{c,k}$, its maximum value is attained when this constraint is satisfied with equality. In other words, at the optimum, the entire available common rate should be fully utilized. Therefore, the optimal common-rate allocation can be chosen as an equal distribution among all users, i.e., $r_{c,k}^* = \frac{1}{K}\min_k\{R_{c,k}\}, \forall k$, where $(\cdot)^*$ denotes the optimal value.

B. Transformation Based on FP

In this section, the FP method [17] is employed to transform the intractable non-convex objective function (6a) and constraints (6d) into a more tractable form. By substituting the optimal common rate into (**P1**) and applying the FP-based reformulation, an equivalent problem, denoted as (**P3**), can be obtained as:

$$
\begin{aligned}
(\mathbf{P3}) \max_{\mathbf{W},\mathbf{\Phi},\mathbf{x},\boldsymbol{\mu},\boldsymbol{\epsilon},\boldsymbol{\gamma},\mathbf{v},y} \quad & \sum_{k=1}^{K} \Psi_k(\boldsymbol{\mu},\boldsymbol{\epsilon},\mathbf{W},\mathbf{x},\mathbf{\Phi}) + y && \text{(7a)}\\
\text{s.t.} \quad & T_k(\boldsymbol{\gamma},\mathbf{v},\mathbf{W},\mathbf{\Phi},\mathbf{x}) \ge y, \quad \forall k, && \text{(7b)}\\
& \Psi_k(\boldsymbol{\mu},\boldsymbol{\epsilon},\mathbf{W},\mathbf{x},\mathbf{\Phi}) \ge \iota, \quad \forall k, && \text{(7c)}\\
& \text{(6b), (6g), (6h)}
\end{aligned}
$$

where y is a slack variable introduced to replace $\min_k\{R_{c,k}\}$ [16], and $\boldsymbol{\mu} = [\mu_1, \cdots, \mu_K]^T$, $\boldsymbol{\epsilon} = [\epsilon_1, \cdots, \epsilon_K]^T$, $\boldsymbol{\gamma} = [\gamma_1, \cdots, \gamma_K]^T$, $\mathbf{v} = [v_1, \cdots, v_K]^T$ are auxiliary variables introduced by the FP technique. The functions Ψ_k and T_k are given in (13) and (14).

1) Updating Auxiliary Variables $\boldsymbol{\mu}$, $\boldsymbol{\gamma}$, $\boldsymbol{\epsilon}$, $\boldsymbol{v}$: It is noteworthy that when other variables are fixed, equations (13) and (14) are concave functions with respect to the auxiliary variables. Consequently, their updates can be obtained by taking the corresponding derivatives. The updates of auxiliary variables are given in (15)∼(18) in [18]. They are ignored here for simplicity.

2) Updating Beamforming Matrix **W** *and Slack Variable y:* With other variables fixed, the problem (**P3**) can be reformulated as:

$$
(\mathbf{P3.1}) \max_{\mathbf{W},y} \sum_{k=1}^{K} \Psi_k(\mathbf{W}) + y \quad \text{s.t. (6b), (7b), (7c)}
$$

This is a convex problem. Although tools such as CVX can solve it effectively, they incur higher complexity. Therefore, in this subsection, we adopt the algorithm in [16] to solve

the beamforming matrix via the KKT conditions. The update formula for the beamforming matrix $\mathbf{W}$ is given by:

$$\mathbf{w}_c^* = \left(\sum_{k=1}^{K} \lambda_k^* |v_k|^2 \mathbf{h}_k(\mathbf{x})\mathbf{h}_k^H(\mathbf{x}) + \kappa^* \mathbf{I}\right)^{-1} \sum_{k=1}^{K} (\lambda_k^* \sqrt{1+\gamma_k}\, v_k \mathbf{h}_k(\mathbf{x})) \tag{9a}$$

$$\mathbf{w}_m^* = \left(\sum_{k=1}^{K} (|\epsilon_k|^2(1+\eta_k) + \lambda_k^*|v_k|^2)\mathbf{h}_k(\mathbf{x})\mathbf{h}_k^H(\mathbf{x}) + \kappa^* \mathbf{I}\right)^{-1} 2(1+\eta_m)\sqrt{1+\mu_m}\, \epsilon_m\, \mathbf{h}_m(\mathbf{x}),\ \forall m \neq c, \tag{9b}$$

where $\boldsymbol{\lambda} = [\lambda_1, \cdots, \lambda_K]^T$, κ and $\boldsymbol{\eta} = [\eta_1, \cdots, \eta_K]$ are the Lagrange multipliers associated with constraints (7b) , (6b) and (7c), respectively. Among them, $\mathbf{I}$ is the identity matrix, equations (9a) and (9b) arise from stationary condition. According to the structure of problem (**P3.1**), the optimal value of y is $y^* = T_z(\mathbf{W})$, where z denotes the user index corresponding to $\min_k\{T_k\}$. Applying the fixed point iteration method in [16], the update rules for the Lagrange multipliers can be derived as follows:

$$\lambda_k^{[t+1]} = \frac{T_z(\mathbf{W})+\rho}{T_k(\mathbf{W})+\rho}\lambda_k^{[t]}, \quad \forall k \neq z, \tag{10a}$$

$$\lambda_z^{[t+1]} = \lambda_z^{[t]} + \sum_{k=1}^{K}\left(\lambda_k^{[t]} - \frac{T_z(\mathbf{W})+\rho}{T_k(\mathbf{W})+\rho}\lambda_k^{[t]}\right), \tag{10b}$$

$$\eta_k^{[t+1]} = \frac{\Psi_k(\mathbf{W})+\rho}{\iota+\rho}, \tag{10c}$$

$$\kappa^{[t+1]} = \frac{\mathrm{tr}(\mathbf{W}\mathbf{W}^H)+\rho}{P_T+\rho}, \tag{10d}$$

where constant $\rho \geq 0$ is employed to enhance convergence stability by effectively reducing the step size. $(\cdot)^{[t]}$ and $(\cdot)^{[t+1]}$ are the value of t-th and $(t+1)$-th iteration respectively. Equation (10b) is designed to ensure that the KKT condition (10d) is satisfied during iteration.

3) Updating RIS Reflection Matrix $\mathbf{\Phi}$: In this subsection, we present a low-complexity iterative algorithm for updating the RIS reflection matrix $\mathbf{\Phi}$. The equivalent channel vector from the BS to user k can be simplified as $\mathbf{h}_k^H(\mathbf{x}) = \boldsymbol{\phi}^H\mathbf{U}_k + \mathbf{u}_k^H$, where $\boldsymbol{\phi} = \mathrm{diag}(\mathbf{\Phi}^H)$, $\mathbf{U}_k = \mathrm{diag}(\mathbf{h}_{r,k}^H)\mathbf{B}^H\mathbf{\Sigma}\mathbf{A}$, $\mathbf{u}_k = \mathbf{A}_k^H\mathbf{\Sigma}_k\mathbf{1}$. By substituting the simplified channel vector into problem (**P3**) and fixing other variables, we obtain:

$$(\mathbf{P3.2})\ \max_{\boldsymbol{\phi}}\quad -\boldsymbol{\phi}^H\mathbf{M}_1\boldsymbol{\phi} + \Re\Big\{\boldsymbol{\phi}^H(\mathbf{M}_2 - 2\mathbf{M}_3)\Big\} \tag{11a}$$

$$\text{s.t.}\quad (6f),$$

$$-\boldsymbol{\phi}^H\mathbf{C}_{1,k}\boldsymbol{\phi} + \Re\{\boldsymbol{\phi}^H(\mathbf{C}_{2,k} - 2\mathbf{C}_{3,k})\} \geq c_k,\ \forall k, \tag{11b}$$

$$\sum_{k=1}^{K} r_{c,k} \leq -\boldsymbol{\phi}^H\mathbf{N}_{1,k}\boldsymbol{\phi} + \Re\Big\{\boldsymbol{\phi}^H(\mathbf{N}_{2,k} - \mathbf{N}_{3,k})\Big\} + d,\ \forall k, \tag{11c}$$

where $\mathbf{C}_{1,k}{=}\mathbf{U}_k(|\epsilon_k|^2\sum_{i=1}^K \mathbf{w}_i\mathbf{w}_i^H)\mathbf{U}_k^H$, $\mathbf{C}_{2,k}{=}2\sqrt{1+\mu_k}\bar{\epsilon}_k\mathbf{U}_k\mathbf{w}_k$, $\mathbf{C}_{3,k}{=}\mathbf{U}_k(|\epsilon_k|^2\sum_{i=1}^K \mathbf{w}_i\mathbf{w}_i^H)\mathbf{u}_k$, $\mathbf{N}_{1,k}{=}|v_k|^2\mathbf{U}_k(\mathbf{w}_c\mathbf{w}_c^H + \sum_{i=1}^K \mathbf{w}_i\mathbf{w}_i^H)\mathbf{U}_k^H$, $\mathbf{N}_{2,k}{=}2\sqrt{1+\mu_k}\bar{v}_k\mathbf{U}_k\mathbf{w}_c$, $\mathbf{N}_{3,k}{=}2|v_k|^2\mathbf{U}_k(\mathbf{w}_c\mathbf{w}_c^H - \sum_{i=1}^K \mathbf{w}_i\mathbf{w}_i^H)\mathbf{u}_k$, $\mathbf{M}_1{=}\sum_{k=1}^K \mathbf{C}_{1,k}$, $\mathbf{M}_2{=}\sum_{k=1}^K \mathbf{C}_{2,k}$, $\mathbf{M}_3{=}\sum_{k=1}^K \mathbf{C}_{3,k}$, $d{=}2\sqrt{1+\gamma_k}\Re\{\bar{v}_k\mathbf{u}_k^H\mathbf{w}_c\} - |v_k|^2\mathbf{u}_k^H\sum_i \mathbf{w}_i\mathbf{w}_i^H\mathbf{u}_k$, $c_k{=}\iota{+}\mu_k{-}\log_2(1{+}\mu_k){-}2\sqrt{1+\mu_k}\Re\{\bar{\epsilon}_k\mathbf{u}_k^H\mathbf{w}_k\}{+}|\epsilon_k|^2\mathbf{u}_k^H\sum_i \mathbf{w}_i\mathbf{u}_k$. The dual problem of (**P3.2**) is given by:

$$(\mathbf{P3.2.1})\ \max_{\boldsymbol{\xi}}\ \min_{\boldsymbol{\phi}}\ \mathcal{L}(\boldsymbol{\phi}, \boldsymbol{\xi}, \boldsymbol{\varpi}) \quad \text{s.t. (6f)}$$

where $\mathcal{L}(\boldsymbol{\phi}, \boldsymbol{\xi}, \boldsymbol{\varpi})$ is the Lagrangian function corresponding to (**P3.2**). $\boldsymbol{\xi} = [\xi_1, \xi_2, ..., \xi_K]^T$ and $\boldsymbol{\varpi} = [\varpi_1, \cdots, \varpi_K]^T$ denote the Lagrange multiplier corresponding to (11c) and (11b) respectively. We employ the dual ascent method to solve this problem. First, the Lagrange multipliers are fixed to update $\boldsymbol{\phi}$. Combining with (6f) and Lemma 1 in [19], we can derive an upper-bound function in place of the Lagrangian function as $\Re\{\boldsymbol{\phi}^H\mathbf{h}\}$, where $\mathbf{h} = 2(\mathbf{M_1} + \sum_{i=1}^K \xi_i\mathbf{N}_{1,i} + \sum_{i=1}^K \varpi_i\mathbf{C}_{1,i} - \lambda_{max}\mathbf{I})\boldsymbol{\phi}^{[t]} - (\mathbf{M}_2 - 2\mathbf{M}_3 + \sum_{i=1}^K \xi_i(\mathbf{N}_{2,i} - \mathbf{N}_{3,i}) + \sum_{i=1}^K \varpi_i(\mathbf{C}_{2,i} - 2\mathbf{C}_{3,i}))$, λ_{max} is the maximum eigenvalue of matrix $\mathbf{M}_1 + \sum_{i=1}^K \xi_i\mathbf{N}_{1,i} + \sum_{i=1}^K \varpi_i\mathbf{C}_{1,i}$. In addition, the gradient ascent method is employed to update $\boldsymbol{\xi}$. The update formulas for $\boldsymbol{\xi}$ and $\boldsymbol{\phi}$ are given as follows:

$$\xi_i^{[t+1]} = \left[\xi_i^{[t]} + \left(\sum_{k=1}^{K} r_{c,k} + (\boldsymbol{\phi}^{[t]})^H\mathbf{N}_{1,i}\boldsymbol{\phi}^{[t]} - \Re\Big\{(\boldsymbol{\phi}^{[t]})^H(\mathbf{N}_{2,i} - \mathbf{N}_{3,i})\Big\} - d\right)\tau\right]^+, \tag{15a}$$

$$\varpi_i^{[t+1]} = \left[\varpi_i^{[t]} + \left(c_i + (\boldsymbol{\phi}^{[t]})^H\mathbf{C}_{1,i}\boldsymbol{\phi}^{[t]} - \Re\Big\{(\boldsymbol{\phi}^{[t]})^H(\mathbf{C}_{2,i} - 2\mathbf{C}_{3,i})\Big\}\right)\tau\right]^+, \tag{15b}$$

$$\mathbf{\Phi}^{[t+1]} = \mathrm{diag}(-e^{j\angle\mathbf{h}}). \tag{15c}$$

where τ is the step size for gradient ascent and can be set to a small fixed value. $[\cdot]^+ = \max\{0, \cdot\}$ is the projection function for the Lagrange multiplier $\boldsymbol{\xi}$.

4) Updating MA Positions: With other variables fixed, we can get the subproblem as follows:

$$(\mathbf{P3.3})\ \max_{\mathbf{x}}\ \Psi(\mathbf{x}) = \sum_{k=1}^{K}\Psi_k(\mathbf{x}) \tag{16a}$$

$$\text{s.t.}\ \ T_k(\mathbf{x}) \geq y,\ \forall k \tag{16b}$$

$$(6g),\ (6h), (7c)$$

Considering the non-convex nature of this problem, we employ the gradient ascent method to update the positions of the MA. The gradient of the objective function with respect to x_m is denoted as $\nabla_{x_m}\Psi(\mathbf{x})$. Accordingly, the position of the m-th MA is updated as follows:

$$x_m^{[t+1]} = x_m^{[t]} + \alpha(\nabla_{x_m}\Psi_1(\mathbf{x}) + \nabla_{x_m}\Psi_2(\mathbf{x})), \forall m \tag{17}$$

where $\Psi_1(\mathbf{x}) = \sum_{k=1}^K \Psi_{k,1}(\mathbf{x})$ and $\Psi_2(\mathbf{x}) = \sum_{k=1}^K \Psi_{k,2}(\mathbf{x})$. α denotes the step size of the gradient ascent iteration. Even if a feasible initial solution is selected, the gradient ascent procedure may still violate the feasible region during the iteration process. In such cases, the step size α is reduced to 0.5α to

$$\Psi_k(\cdot) = \log_2(1+\mu_k) - \mu_k + \underbrace{2\sqrt{1+\mu_k}\,\Re\{\bar{\epsilon}_k \mathbf{h}_k^H(\mathbf{x})\mathbf{w}_k\}}_{\Psi_{k,1}} - \underbrace{|\epsilon_k|^2\left(\sum_{i=1}^{K}|\mathbf{h}_k^H(\mathbf{x})\mathbf{w}_i|^2 + \sigma_k^2\right)}_{\Psi_{k,2}} \tag{13}$$

$$T_k(\cdot) = \log_2(1+\gamma_k) - \gamma_k + 2\sqrt{1+\gamma_k}\,\Re\{\bar{v}_k \mathbf{h}_k^H(\mathbf{x})\mathbf{w}_c\} - |v_k|^2\left(|\mathbf{h}_k^H(\mathbf{x})\mathbf{w}_c|^2 + \sum_{i=1}^{K}|\mathbf{h}_k^H(\mathbf{x})\mathbf{w}_i|^2 + \sigma_k^2\right) \tag{14}$$

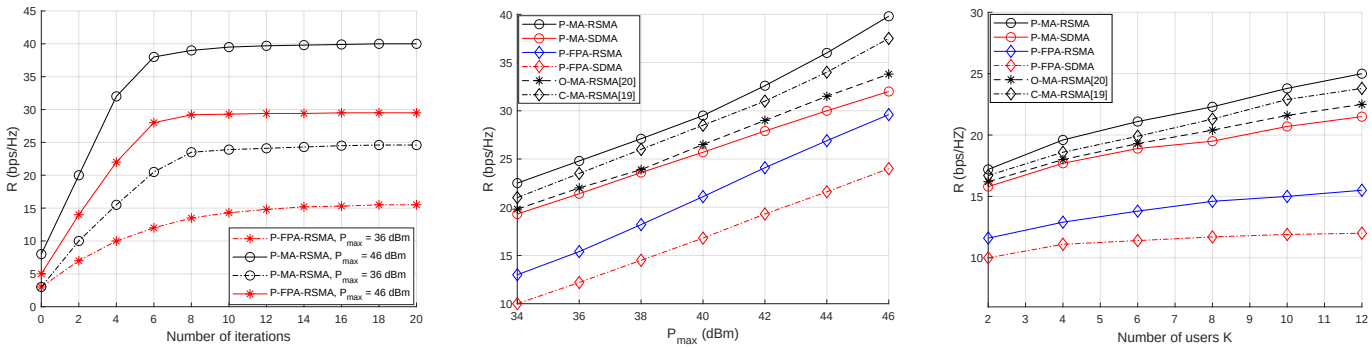

(a) Iteration number versus sum rate (b) Power budget versus sum rate (c) Number of users versus sum rate

Fig. 2: Performance comparison under different conditions

ensure that the updated position remains within the feasible set R_f, where R_f is the feasible region for problem (**P3.3**). The gradients of $\Psi_1(\mathbf{x})$ and $\Psi_2(\mathbf{x})$ are omitted for brevity. Also, gradient ascent algorithms for updating MA positions have been introduced in many articles like the **Algorithm 2** in [18].Therefore, we do not elaborate on them here. The overall algorithm for solving problem (**P1**) is displayed in **Algorithm 1**.

C. Complexity Analysis

The computational complexity of gradient ascent for updating MA positions is approximately $\mathcal{O}(N_G M^2 K^2 L_t^2)$, where N_G is the total number of gradient ascent iterations. In **Algorithm 1**, the complexities of updating the FP parameters and Lagrange multipliers are $\mathcal{O}(8M)$ and $\mathcal{O}(2M(K+1)+K)$, respectively. For the beamforming matrix update, LU decomposition is employed to reduce inversion complexity, requiring only one LU factorization, while the subsequent inverse computations incur a complexity of $\mathcal{O}(M^2)$. Therefore, assuming the total number of outer iterations is N_T, the overall computational complexity of the proposed algorithm is approximately $\mathcal{O}\big(M^3 + N_T(8M + 2M(K+1) + K + M^2 + N_G M^2 K^2 L_t^2)\big)$.

IV. Numerical Results

In this section, we evaluate the performance of the proposed MA-assisted RSMA-RIS algorithm (P-MA-RSMA) and compare it with the CFGS-based MA-RSMA scheme (C-MA-RSMA) [18] and the ORIS-RSMA scheme (O-MA-RSMA) [20]. We also include the MA-aided SDMA-RIS scheme (P-MA-SDMA) and the FPA-based RSMA-RIS (P-FPA-RSMA) and SDMA-RIS (P-FPA-SDMA) schemes for comparison.

Algorithm 1 AO for Solving Problem (**P1**)

Initialization: Set $\{\boldsymbol{\lambda}^{[t]}, \kappa^{[t]}, \boldsymbol{\eta}^{[t]}, \boldsymbol{\mu}^{[t]}, \boldsymbol{\epsilon}^{[t]}, \boldsymbol{v}^{[t]}, \boldsymbol{\gamma}^{[t]}, \mathbf{W}^{[t]}, \mathbf{x}^{[t]}, \boldsymbol{\Phi}^{[t]}, \boldsymbol{\xi}^{[t]}, \boldsymbol{\varpi}^{[t]}, \{r_{c,k}^{[t]}\}\}$. Set iteration index $t = 0$, maximum iteration number $t_{\max}$, and threshold ϵ. Calculate $\{R^{[t]}, \{R_{c,k}^{[t]}\}, \{T_k^{[t]}\}\}$ by (6a), (3), (14) respectively.
repeat
  Update $\boldsymbol{\mu}^{[t+1]}$, $\boldsymbol{\epsilon}^{[t+1]}$, $\boldsymbol{v}^{[t+1]}$, $\boldsymbol{\gamma}^{[t+1]}$ by (15)$\sim$ (18) in [18].
  Update $\boldsymbol{\lambda}^{[t+1]}$, $\kappa^{[t+1]}$, $\boldsymbol{\eta}^{[t+1]}$ by (10a)$\sim$(10d).
  Update $\mathbf{W}^{[t+1]}$ by (9a) and (9b).
  Calculate $\{R_{c,k}^{[t+1]}\}$ and update $\{r_{c,k}^{[t+1]}\}$ by $\{r_{c,k}^{[t+1]}\} = \frac{1}{K}\min\{R_{c,k}^{[t+1]}\}, \forall k$.
  Update $\boldsymbol{\xi}^{[t+1]}$,$\boldsymbol{\varpi}^{[t+1]}$ and $\boldsymbol{\Phi}^{[t+1]}$ by (15a) and (15c).
  Update $\mathbf{x}^{[t+1]}$ by **Algorithm 2** in [18].
  Calculate $R^{[t+1]}$, $\{T_k^{[t+1]}\}$ and set $t = t+1$.
until $|R^{[t+1]} - R^{[t]}| < \epsilon$ or $t \geq t_{\max}$
Output: $R^{[t+1]}$.

Unless otherwise specified, the simulation parameters are set as follows. The numbers of transmit and receive paths are $L_t = L_r = L = 4$, and the elevation and azimuth angles of all paths are uniformly distributed over $[0, \pi]$. The BS employs $M = 16$ antennas, and the RIS has $N = 32$ reflecting elements. The carrier frequency is $f = 3 \times 10^9$ Hz [18], and the wavelength is $\lambda = \frac{c}{f}$, where c is the speed of light. The user rate threshold is set to $\iota = 1$ bit/s. Each movable antenna can move within $[-6\lambda, 6\lambda]$, with a minimum adjacent spacing of $\lambda/2$. The noise power is -80 dBm. The BS array center and RIS are located at $(0\,\mathrm{m}, 0\,\mathrm{m})$ and $(12\,\mathrm{m}, 16\,\mathrm{m})$, respectively, while users are uniformly dis-

tributed in $[20\,\mathrm{m}, 40\,\mathrm{m}] \times [0\,\mathrm{m}, -20\,\mathrm{m}]$. Due to obstacles, no LoS path exists between the BS and users, whereas the BS–RIS and RIS–user links are LoS. Accordingly, the diagonal entries of the BS–user fading matrix $\mathbf{\Sigma}_k$ are modeled as $\mathbf{\Sigma}_k[i,i] \sim \mathcal{CN}\Big(0, \frac{1}{p+1} C_0 \left(\frac{d_0}{d_k}\right)^{\alpha_1} / L\Big)$, $\forall k, \forall i$ [21], where $C_0 = \left(\frac{\lambda}{4\pi}\right)^2$, d_0 is the unit reference distance, and d_k is the distance between the BS and user k. For the BS–RIS channel $\mathbf{\Sigma}$, the diagonal entries are given by $\mathbf{\Sigma}[1,1] \sim \mathcal{CN}\Big(0, \frac{p}{p+1} C_0 \left(\frac{d_0}{d_{br}}\right)^{\alpha_c}\Big)$ and $\mathbf{\Sigma}[i,i] \sim \mathcal{CN}\Big(0, \frac{1}{p+1} C_0 \left(\frac{d_0}{d_{br}}\right)^{\alpha_c} / (L-1)\Big)$, $\forall i \neq 1$, where the Rician factor is $p = 0.5$, $c \in \{2, 3\}$ corresponds to the BS–RIS and RIS–user links, respectively, and d_{br} is the BS–RIS distance. The path-loss exponents are set to $\alpha_1 = 3.5$, $\alpha_2 = 2.5$, and $\alpha_3 = 2.5$ [21].

First, Fig. 2(a) analyzes the evolution of the RSMA sum rate versus the iteration index under two transmit-power constraints. Across all four schemes, the curves converge in approximately 10 iterations and then remain stable, with the higher-power setting reaching a larger steady-state sum rate.

Then, we investigate how the sum rate R scales with the maximum transmit power $P_{\max}$ in Fig. 2(b). The number of users is set to $K = 12$. It can be observed that the performance of the proposed algorithm in this work is superior to the algorithms in [18], [20]. As expected, R increases monotonically with $P_{\max}$, and the slope for RSMA is larger than that for SDMA. Specifically, as the power budget increases from 34 dBm to 46 dBm, the sum rate of MA-RSMA increases by approximately 81.8%, while that of MA-SDMA increases by only approximately 64.1%. This is because RSMA affords higher degrees of freedom (DoF) than SDMA [10]. Furthermore, it can be observed that both SDMA-RIS and RSMA-RIS systems achieve significant performance gains with the incorporation of MA. Specifically, MA provides approximately a 35.6% performance enhancement for the RSMA system, compared to about 33.3% for the SDMA system at 46dBm.

In Fig. 2(c), we examine the relationship between the number of users K and the sum rate. The power budget is set to 36dBm. Overall, the sum rate increases with K. As the number of users increases from 2 to 12, the sum rate of MA-RSMA increases by approximately 47.1%, while that of FPA-RSMA increases by only approximately 29.2%.

V. Conclusion

In this work, we investigate the MA assisted RSMA–RIS downlink MISO system and maximize the sum rate via joint optimization of the transmit beamforming matrix, the common-rate allocation, the RIS reflection matrix, and the MA positions. We develop an efficient solution based on a FP reformulation to solve this problem. Numerical results demonstrate that, our proposed algorithm can effectively solve the initial probelm and prove that MA can improve the performance of RSMA–RIS system.

References

[1] L. Zhu, W. Ma, and R. Zhang, "Modeling and performance analysis for movable antenna enabled wireless communications," *IEEE Transactions on Wireless Communications*, vol. 23, no. 6, pp. 6234–6250, 2023.

[2] S. Nithya, T. Jagadesh, E. Shalini, T. Sathiyapriya, V. Teresa, and P. R. Buvaneswari, "Design and development of movable antenna system for multiplatform wireless communication," in *2022 IEEE 2nd Mysore Sub Section International Conference (MysuruCon)*. IEEE, 2022, pp. 1–5.

[3] W. Ma, L. Zhu, and R. Zhang, "Mimo capacity characterization for movable antenna systems," *IEEE Transactions on Wireless Communications*, vol. 23, no. 4, pp. 3392–3407, 2023.

[4] G. Yan, L. Zhu, and R. Zhang, "Movable antenna aided multiuser communications: Antenna position optimization based on statistical channel information," *arXiv preprint arXiv:2502.20856*, 2025.

[5] L. Zhu, W. Ma, B. Ning, and R. Zhang, "Movable-antenna enhanced multiuser communication via antenna position optimization," *IEEE Transactions on Wireless Communications*, vol. 23, no. 7, pp. 7214–7229, 2023.

[6] Y. Cang, M. Chen, and Z. Yang, "Movable antenna enhanced mec systems with discrete antenna position selection," *IEEE Communications Letters*, 2025.

[7] P. Liu, J. Si, Z. Cheng, Z. Li, and H. Hu, "Movable-antenna enabled covert communication," *IEEE Wireless Communications Letters*, 2024.

[8] Y. Mao, B. Clerckx, and V. O. Li, "Rate-splitting multiple access for downlink communication systems: Bridging, generalizing, and outperforming sdma and noma," *EURASIP journal on wireless communications and networking*, vol. 2018, no. 1, p. 133, 2018.

[9] C. Hao, Y. Wu, and B. Clerckx, "Rate analysis of two-receiver miso broadcast channel with finite rate feedback: A rate-splitting approach," *IEEE Transactions on Communications*, vol. 63, no. 9, pp. 3232–3246, 2015.

[10] Y. Mao, O. Dizdar, B. Clerckx, R. Schober, P. Popovski, and H. V. Poor, "Rate-splitting multiple access: Fundamentals, survey, and future research trends," *IEEE communications surveys & tutorials*, vol. 24, no. 4, pp. 2073–2126, 2022.

[11] C. Hao, B. Rassouli, and B. Clerckx, "Achievable dof regions of mimo networks with imperfect csit," *IEEE Transactions on Information Theory*, vol. 63, no. 10, pp. 6587–6606, 2017.

[12] E. Piovano and B. Clerckx, "Optimal dof region of the k-user miso bc with partial csit," *IEEE Communications Letters*, vol. 21, no. 11, pp. 2368–2371, 2017.

[13] Q. Wu and R. Zhang, "Intelligent reflecting surface enhanced wireless network via joint active and passive beamforming," *IEEE transactions on wireless communications*, vol. 18, no. 11, pp. 5394–5409, 2019.

[14] C. Huang, A. Zappone, G. C. Alexandropoulos, M. Debbah, and C. Yuen, "Reconfigurable intelligent surfaces for energy efficiency in wireless communication," *IEEE transactions on wireless communications*, vol. 18, no. 8, pp. 4157–4170, 2019.

[15] Z. Yang, M. Chen, W. Saad, W. Xu, M. Shikh-Bahaei, H. V. Poor, and S. Cui, "Energy-efficient wireless communications with distributed reconfigurable intelligent surfaces," *IEEE Transactions on Wireless Communications*, vol. 21, no. 1, pp. 665–679, 2021.

[16] T. Fang and Y. Mao, "Rate splitting multiple access: Optimal beamforming structure and efficient optimization algorithms," *IEEE Transactions on Wireless Communications*, 2024.

[17] K. Shen and W. Yu, "Fractional programming for communication systems—part i: Power control and beamforming," *IEEE Transactions on Signal Processing*, vol. 66, no. 10, pp. 2616–2630, 2018.

[18] C. Zhang, S. Peng, Y. Xu, Q. Wu, X. Ou, X. Guo, D. He, and W. Zhang, "Sum rate maximization for movable antenna-aided downlink rsma systems," in *ICC 2025 - IEEE International Conference on Communications*, 2025, pp. 1049–1054.

[19] C. Huang, A. Zappone, G. C. Alexandropoulos, M. Debbah, and C. Yuen, "Reconfigurable intelligent surfaces for energy efficiency in wireless communication," *IEEE Transactions on Wireless Communications*, vol. 18, no. 8, pp. 4157–4170, 2019.

[20] A. Qayyum and M. Nekovee, "Power allocation and ris elements optimisation for reconfigurable intelligent surfaces assisted rsma," *arXiv preprint arXiv:2507.17419*, 2025.

[21] H. Wu, H. Ren, C. Pan, and Y. Zhang, "Movable antenna-enabled ris-aided integrated sensing and communication," *IEEE Transactions on Cognitive Communications and Networking*, 2025.